Catena 196 (2021) 104913

Contents lists available at ScienceDirect

Catena

journal homepage: www.elsevier.com/locate/catena

Millennial-scale terrestrial ecosystem responses to Upper Pleistocene climatic changes: 4D-reconstruction of the Schwalbenberg Loess-Palaeosol-Sequence (Middle Rhine Valley, Germany)

Peter Fischer[a,*], Olaf Jöris[b], Kathryn E. Fitzsimmons[c], Mathias Vinnepand[a], Charlotte Prud'homme[c], Philipp Schulte[d], Christine Hatté[e], Ulrich Hambach[f], Susanne Lindauer[g], Christian Zeeden[h], Zoran Peric[c], Frank Lehmkuhl[d], Tina Wunderlich[i], Dennis Wilken[i], Wolfgang Schirmer[j], Andreas Vött[a]

[a] Institute of Geography, Johannes Gutenberg University Mainz, Johann-Joachim-Becher-Weg 21, 55099 Mainz, Germany
[b] MONREPOS Archaeological Research Centre and Museum for Human Behavioural Evolution, RGZM, Schloss Monrepos, 56567 Neuwied, Germany
[c] Research Group for Terrestrial Palaeoclimates, Max Planck Institute for Chemistry, Hahn-Meitner-Weg 1, 55128 Mainz, Germany
[d] Department of Geography, Chair of Physical Geography and Geoecology, RWTH Aachen University, Wüllnerstrasse 5b, 52056 Aachen, Germany
[e] Laboratoire des Sciences du Climat et de l'Environnement, UMR 8212 CNRS CEA UVSQ, Université Paris-Saclay, 91198 Gif-sur-Yvette, France
[f] BayCEER & Chair of Geomorphology, University of Bayreuth, 95440 Bayreuth, Germany
[g] Curt-Engelhorn-Centre of Archeometry, 68159 Mannheim, Germany
[h] Leibniz Institute for Applied Geophysics, Stilleweg 2, 30655 Hannover, Germany
[i] Applied Geophysics, Christian-Albrechts-University of Kiel, 24118 Kiel, Germany
[j] Wolkenstein 24, 91320 Ebermannstadt, Germany

ARTICLE INFO

Keywords:
Loess-Palaeosol-Sequence
Upper Pleistocene
Schwalbenberg
Middle Rhine
North Atlantic Climate Oscillations

ABSTRACT

Loess-Palaeosol-Sequences (LPS) in the Central European region provide outstanding terrestrial polygenetic and multiphase archives responding to past climate and environments over various spatial and temporal scales. As yet, however, the geomorphological and pedogenic processes involved in LPS formation, and their interplay with changes in ecological conditions, impede robust correlation with other palaeoenvironmental archives. The Schwalbenberg LPS, which drape a hillslope in the Middle Rhine Valley in western Central Europe, provide unique high-resolution records highly suitable for investigating the processes involved in their formation and the relationship to climatic influences during the Upper Pleistocene. Here we present the first comprehensive multi-proxy dataset for the Schwalbenberg LPS over four dimensions. We undertake systematic analyses along a representative slope transect using surface-based geophysical prospection in combination with Direct Push hydraulic profiling to characterise the subsurface stratigraphy in detail. We integrate selected sedimentological and geochemical proxy data from three long sediment cores and two profile sections to build a complete stratigraphical succession for the Schwalbenberg LPS. We show that the transect approach allows quantification of different formation phases, whether accumulative, erosive or pedogenic in character. In so doing we overcome the bias inherent in studies of individual sections and enable robust and reliable correlation with other climate archives. For the time interval ~ 80–15 ka BP correlation of combined lithostratigraphic features and organic carbon contents from Schwalbenberg with the Sofular and NGRIP $\delta^{18}O$-records can be established at millennial to centennial scale resolution, highlighting the sensitivity of western European LPS to the Atlantic-driven climate oscillations in much more detail than in any other terrestrial archive known in the region so far.

1. Introduction

Loess sediments are the most extensive palaeoenvironmental archives of the Quaternary Period. They are especially widespread across northern Eurasia (e.g. Haase et al., 2007; Pecsi and Richter, 1995; Rousseau et al., 2018, 2017a) and can exceed 200 m thickness, as in the case of the Chinese Loess Plateau (e.g. Kukla and An, 1989). The dominantly silt-sized mineral grains, from which loess sediments are

* Corresponding author.
E-mail address: p.fischer@geo.uni-mainz.de (P. Fischer).

https://doi.org/10.1016/j.catena.2020.104913
Received 30 May 2020; Received in revised form 31 August 2020; Accepted 6 September 2020

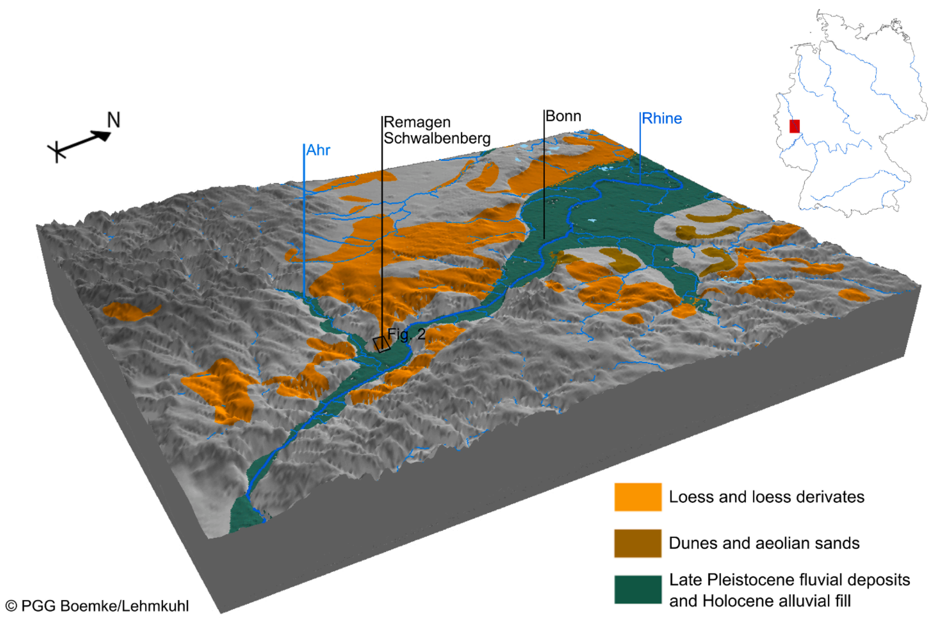

Fig. 1. Block diagram of the Lower Middle Rhine valley including Remagen-Schwalbenberg and the transition to the Lower Rhine Embayment. The Schwalbenberg site is located northwest of the Ahr River mouth into the Rhine River. Size of the 3D-image is 40 × 55 km. Superelevated by factor 1 (no superelevation). Geodata: (Lehmkuhl et al., 2018) and ALOS digital elevation model (JAXA EORC, n.d).

correlated to the Lower Middle Terrace (LMT; equivalent to t_{r9} after Bibus, 1980; LMT 1 after Boenigk and Frechen, 2006) of the region that has been deposited during the penultimate glaciation. Fluvial gravels reach an overall thickness of 22 m on top of the Devonian bedrock (Bibus, 1980), which is confirmed by Boenigk and Frechen (2006) giving the LMT 1 base at 58 m and its top at 79 m a.s.l. at the same site. The younger LMT 2 is defined as the second sub-stage of the LMT in the lower Middle Rhine area, but has only been described at localities further to the south (Boenigk and Frechen, 2006).

The LPS on top of fluvial deposits described by Bibus (1980) started with a soil sediment which contained the reworked palaeosol of presumably last interglacial age. The overlaying sequence was characterised by approx. 9 m of loess sediments with 8 intercalated brownish soils of different degrees of pedogenic development and thickness, followed by another 3 m of yellowish loess with two intercalated Gelic Gleysols. As Bibus (1980) conducted no further sedimentological and geochronological analyses, the stratigraphic correlation remained vague. In context of regional terrace stratigraphy, it was assumed that the entire LPS at the Schwalbenberg is of last glacial, i.e. Weichselian age.

In subsequent years, sections Schwalbenberg I and II (SB I, II; Figs. 2, S1), were sampled and investigated in great detail. This Rhineward (east to southeast) exposed section was located at a renewed wall of the section studied by Bibus (1980). Likewise, between SB I and SB II the wall was moved back a few meters in the course of further sampling.

Besides detailed litho- and pedostratigraphic descriptions, the investigations comprised luminescence dating (Frechen and Schirmer, 2011), analyses of selected sedimentological and geochemical proxies (grain size distribution, organic carbon and carbonate content, Schirmer, 2012); weathering index deduced from pedogenic oxides and clay contents as well as micromorphology (Schirmer et al., 2012), high resolution XRF scanning (Profe et al., 2016), palaeo- and rock magnetic (Cofflet, 2005), and malacological analyses (Schiermeyer, 2000). The studies demonstrated, that the SB I and II sections preserve the most complete terrestrial record of OIS 3 climate variability in western Central Europe, based on attempts to correlate total organic carbon contents (TOC) with the $\delta^{18}O$ paleoclimate record of Dye 3 and Camp Century (Dansgaard et al., 1984 in Schirmer, 1991), later with the GISP 2 ice core (Grootes and Stuiver, 1997 in Schirmer, 2012) and correlation of the dissolved iron index with the GRIP Summit ice core (Dansgaard et al.,1993 in Schirmer et al., 2012), both supporting the correlation suggested already earlier (Schirmer, 2000; Schirmer, 1991).

Subsequently, Schirmer (2016) defined the Ahr Interstadial Complex with the SB II section as *locus typicus*. It is characterised by 8 soils, 7 Calcaric Cambisols and one Calcaric Regosol, alternating with thin loess and reworked loess layers and Gelic Gleysols. The soils occur – in stratigraphical order from bottom to top – as three soil complexes separated by distinct unconformities: the Lower Remagen Soils (R1 and R2), the Upper Remagen Soils (R3, R4, R5) and the Sinzig Soils S1-S3 (see Supplementary Table ST 1e). While Schirmer (2012) and Schirmer et al. (2012) identify the R3 soil as most intense palaeosol based on the overall TOC maximum and the maximum of the dissolved iron index, Profe et al. (2016) identified soils S1 and S2 as the most intensively weathered palaeosols followed by R3, R2, R1 and R5 based on LOG (Rb/Sr) and LOG (Ba/Sr). However, the palaeosols of the Ahr Interstadial Complex appear as *in-situ* soil formations (Schirmer et al., 2012). Based on the correlation to ice cores, it is estimated to start with Greenland Interstadial (GI) 17 at ~ 58.4 ka BP and ends with GI 5 at ~ 31.5 ka BP following an early GISP 2 age model (Grootes and Stuiver, 1997).

While these correlations appear promising and suggest a first age estimate for the SB II section, such correlations are still lacking reliable chronological tie points, which accounts especially for the lower Ahr Interstadial Complex. High-resolution, multiple aliquot IRSL and thermoluminescence (TL) dating, and three pIR-IRSL ages, yielded a profile with highly scattering age estimates, which did not consistently increase in age with depth (Frechen and Schirmer, 2011). Using both, quartz and feldspar dating from a nearby sediment core (ca. 150 m NNW of SB II; REM 1, Fig. 2), Klasen et al. (2015) likewise observed significant age discrepancies in the lower part of the sequence which were most likely caused by thermally unstable components in the quartz OSL signal. Removal of the thermally unstable components by filtering the signal showed promising agreement with selected pIR-IRSL-dated samples (Klasen et al., 2015) but was not undertaken for all samples within that study. Geochemical analyses suggest that observed variability in luminescence behaviour down-profile is probably caused by changing mineral characteristics. In the upper part of sediment core REM 1, the Eltville Tephra (ET) occurred at 2.15 m b.s., giving an important chronostratigraphical anchor point. Based on Zens et al. (2017) the ET was most likely deposited at 24.3 ± 1.8 ka BP, during the late Greenland Stadial (GS) 3. This age was most recently confirmed by Förster et al. (2020) who linked the ET to a peak in volcanic minerals in the Dehner Maar at 24 300 a BP.

The Schwalbenberg is furthermore of particular importance to

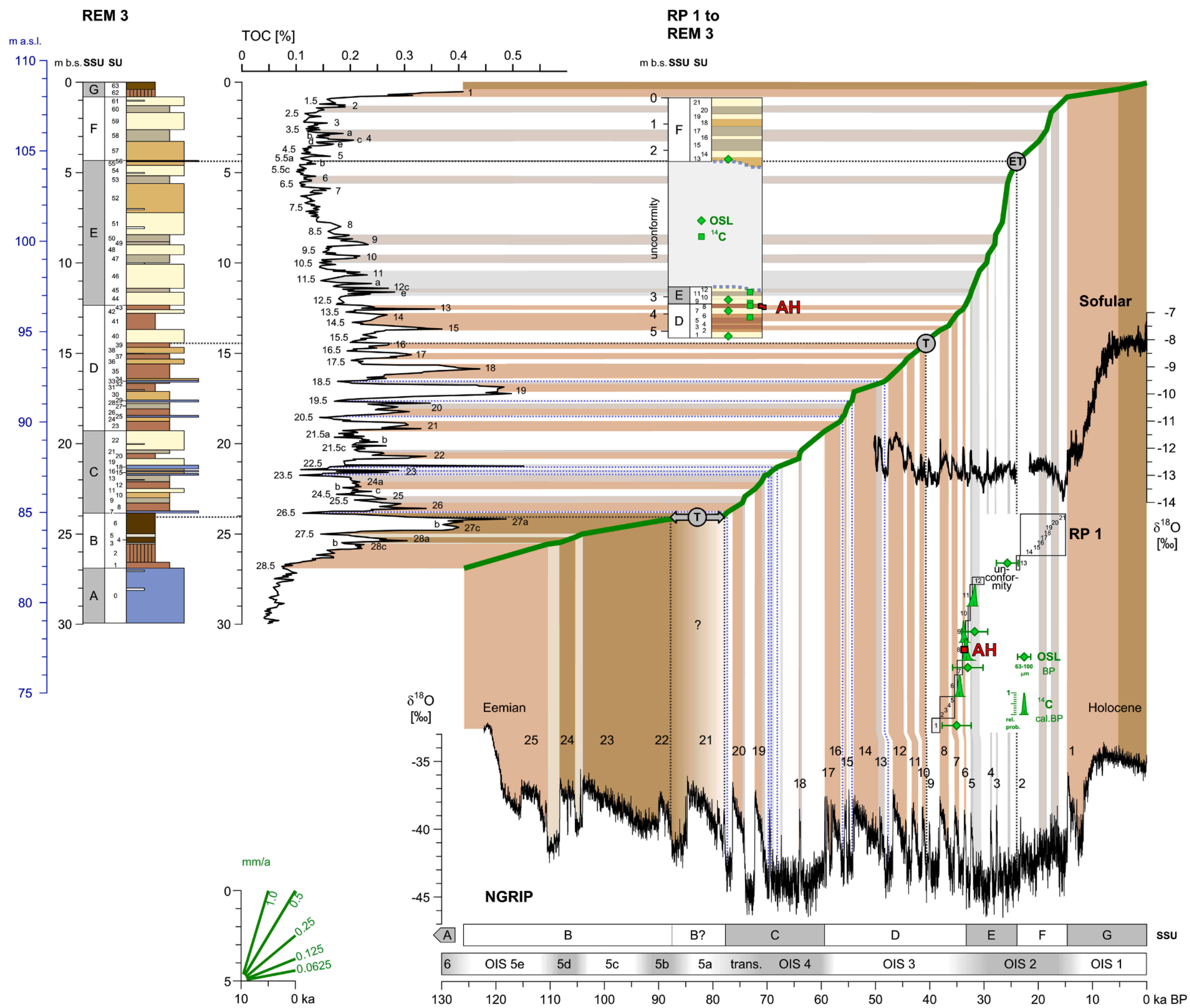

Fig. 11. Depth-age correlation of combined lithostratigraphic features and TOC from sediment core REM 3 to Sofular (Fleitmann et al., 2009) and NGRIP $\delta^{18}O$ records (Rasmussen et al., 2014). OSL and calibrated radiocarbon ages of ECG from the RP 1 profile section and the age of the Eltville Tephra layer (24.3 ka BP; Förster et al., 2020; Zens et al., 2017) represent main anchor points for the correlation and are in overall agreement within their error ranges (cf. Table 4). T and the dotted black lines refer to volcanic material or tephra layers (see discussion in the text). The archaeological horizon (AH) in the uppermost Bw horizon of a Calcaric Cambisol is marked in red. Dotted blue lines represent main erosional unconformities. Brown and greyish bars mark different palaeosols and soil complexes, which form during interstadial and interglacial (lower- and uppermost soils) periods, reflecting changing palaeoclimatic and –environmental conditions at the Schwalbenberg LPS. Depicted OSL ages refer to the Quartz fraction of 63–100 µm, probability distribution of radiocarbon ages is based on CalPal-2007$_{HULU}$ (Weninger and Jöris, 2008). The green line represents the accumulation rate deduced from depth versus age, scale is given in the graph in the lower left corner in mm/a. For legend see Fig. 6, location of sediment core REM 3 in Fig. 2. See Suppl. Fig S28 for enlarged image.

Calcaric Cambisols and reaches comparable thickness in all Schwalbenberg cores and sections. In profile section RP 1 only the upper part of this unit was assessable. In REM 3 and REM 1 coarse-grained layers occur in the lower half of this unit, well depicted in EC and HPT pressure values and clay contents accompanied by distinct minima in TOC contents (REM 3). In contrast, the upper half (above REM 3 SU 33 and REM 1 SU 12) shows no more input of coarse-grained material. In SB II an erosional channel (SB II SU 14) and a small coarser-grained layer (base of SB II SU 16) are also linked to the lower half of unit D. The Bw horizons of SSU D in REM 3 show increasing clay and TOC contents and minima in Ca/Ti from REM 3 SU 23 over REM 3 SU 26 towards REM 3 SU 31, accompanied by HPT pressure values closed to 740 kPa. REM 3 SU 31 is thereby characterised by the absolute maximum of TOC and highest clay contents in unit D, while both proxies decrease above an erosional unconformity indicated by the coarser-grained layer of REM 3 SU 33, but still allowing for a clear differentiation of Bw horizons and intercalated loess and reworked loess. The same decreasing trend is visible in EC and HPT pressure. While Bw horizons of REM 3 SUs 35, 37, 39 are well depicted in clay and TOC contents, they are enclosed in overall higher Ca/Ti-values. This signal is visible in all records despite RP 1, where corresponding SU are not exposed.

The uppermost part of SSU D yields a clear signature now traceable over all investigated records. It is characterised by a thick loess layer (REM 3 SU 40, REM 1 SU 16, REM 5 SU 15, RP 1 SU 1 and SB II SU 29) followed by a tripartite soil complex. In REM 3 and REM 1 this differentiation was not visible during macroscopic core description while soil horizons could be clearly separated in REM 5, RP 1 and SB II. However, proxy-data obviously support the differentiation yielding important anchor points along the whole slope. Notably, in REM 3 at a depth of 14.43 m b.s. platy glass shards were observed at the base of the loess layer of REM 3 SU 40 indicating input of volcanic material.

The next SSU E is developed in all Schwalbenberg cores and sections, showing decreasing thickness downslope. While it contains the characteristic Eltville Tephra (ET tephra) with five separate layers in sediment cores REM 3 and REM 1 at the very top of the unit, this stratigraphic marker is eroded further downslope in REM 5, RP 1 and SB II. Overall, unit E is characterised by calcareous loess and reworked sections, SSU F is relatively thin in REM 1 SU 37. The Gelic Gleysol of REM 3 SU 58 is characterised by a clear peak in TOC values (REM 3 TOCs 4c-4a) and clay concentrations (REM 3 clay 2) and a double-peak in EC (REM 3 ECs 3c-3a). The uppermost Gelic Gleysol (REM 3 SU 60) is only weakly developed and characterised by slightly greyish colours. Downslope, in REM 5 only one candidate for a Gelic Gleysol is observed which cannot be correlated with the other LPS. A peak in clay contents is identified within the reworked loess of REM 5 SU 28. The two Gelic Gleysols on top of the erosional unconformity in section RP 1, namely RP 1 SUs 15 and 17, occur as two peaks in clay contents. The lower one most likely correlates to SB II SU 41. Correlation between Gelic Gleysols along the transect is difficult and suggesting that sediment bleaching and/or oxidation may be highly localised as a result of variable water table levels and episodic waterlogging above permafrost (Antoine et al., 2009).

Following Schirmer (2016) SSU E corresponds to the Hesbaye Member, which typically comprises up to three Gelic Gleysols (named Erbenheim Soils E1-3). It starts above the last brown soil of the Ahr Interstadial Complex and ends within a reworked loess above the ET tephra and below the E4 soil. Based on this, the laminated loess of REM 3 SU 57 below the Gelic Gleysol of REM 3 SU 58 would mark the border to the following Brabant-Member. The Hesbaye unconformity, which often causes truncation of large parts of the OIS 3 successions (e.g. Schirmer, 2016; Fischer et al., 2019) is not observed in the Schwalbenberg LPS. In contrast, a phase of severe erosion leads to a significant truncation of SSU E downslope in REM 5, RP 1 and SB II. Such an erosional event is so far only described for the Lower Rhine area, where it is named Eben unconformity (Schirmer, 2016). SSU E is mainly corresponding to the Late Pleniglacial Brabant Member, which are typically build up by aeolian loess and contain the E4 Gelic Gleysol as important pedostratigraphic marker. REM 3 SU 58 is the most likely correlate to the E4 soil. Following Schirmer (2016, 2013d) the Brabant Member can contain several Gelic Gleysols of different characteristics. However, as mentioned above, a clear stratigraphical identification and correlation of these weakly developed soils of the late Pleniglacial remains vague. In contrast, the Upper Pleniglacial tundra gleys (Gelic Gleysols) at Nussloch are well developed associated to distinct features of periglacial morphodynamics (cp. Antoine et al., 2009), the latter are not observed for the Schwalbenberg.

While at Nussloch loess accumulated in windward position in longitudinal ridges, so-called gredas, trending from NNW to SSE (e.g. Antoine et al., 2001; Gocke et al., 2014) the loess at Schwalbenberg is forming a plateau-like structure in leeward position of the Reisberg trending from W to E with overall low inclination. In both sections, the transition from Weichselian Middle to Upper Pleniglacial is characterised by increasing aeolian dynamics associated to an opening of the landscape and the formation of Gelic Gleysols (Antoine et al., 2009). At Schwalbenberg, however, the Late Glacial is superimposed by pedogenic processes characterising SSU G.

6. Conclusions

We present here the first comprehensive reconstruction of the formation of a loess-palaeosol-sequence in four dimensions, based on the combination of surface-based geophysical prospection, in situ borehole hydraulic and geophysical profiling, sedimentological, geochemical and geochronological data. Based on this approach, we draw the following main conclusions:

I. The loess is underlain by fluvial deposits, which correlate to the Lower Middle Terrace (LMT) 1 and at least two further, as yet unknown, older terrace levels.
II. The LPS increases in thickness from 13 m along the cliffs facing the Ahr and Rhine river valleys, to 27 m in the interfluve position.
III. The LPS preserved in interfluve position (REM 3) provides the most complete record for the Schwalbenberg sequence, and has experienced the least truncation by erosion, in average containing < 5 ka/m. This resolution is exceptional for Upper Pleistocene terrestrial archives.
IV. Correlation of combined lithostratigraphic features and TOC contents from Schwalbenberg with the Sofular and NGRIP δ^{18}O-records suggests for the sequence younger than the OIS 5/4 transition a close match with both the millennial timescales of climatic oscillations as well as the amplitudes of such events. As such, the synthetic Schwalbenberg lithostratigraphic and TOC record can be used to document the sensitivity of western European LPS to northern hemispheric climate oscillations. The Schwalbenberg LPS resolves the Atlantic-driven Upper Pleistocene climate oscillations in more detail than any other terrestrial archive in the region so far.
V. Our multi-proxy correlative approach facilitated the identification of erosional events that would otherwise have remained undetected. Three types of erosion were identified; firstly, surface runoff leading to erosion and subsequent sediment deposition as observed at the OIS 5/4 transition, early OIS 4 and early OIS 3; secondly, truncation in the downslope position, the most pronounced event of which occurred after the deposition of the ET tephra during the late Upper Pleniglacial; and thirdly erosion leading to channel formation and subsequent channel filling.

Overall, our studies at the Schwalbenberg contribute to better understand the mechanisms controlling the interplay of sediment build up, soil formation, sediment relocation and associated preservation of climate signals, resulting in the unique resolution of studied LPS. Recent methodological developments, especially the combination of direct sensing techniques and surface-based geophysical studies accomplished by sedimentological analyses contribute to transfer four-dimensional reconstructions of landscape formation to a larger spatial scale.

Declaration of Competing Interest

The authors declare that they have no known competing financial interests or personal relationships that could have appeared to influence the work reported in this paper.

Acknowledgement

We appreciate funding by the German Research Foundation (Deutsche Forschungs-gemeinschaft, DFG) in the frame of the TERRACLIME-Project (FI 1941/5-1; FI 1918/4-1; VO 938/25-1). Sediment core REM 1 was drilled and analysed in the frame of the CRC 806 “Our Way to Europe”, funded by the DFG (project number 57444011-SFB 806). We thank Barry Thornton for the determination of the TOC content at the James Hutton Institute, Scotland. We also thank Timo Willershäuser (JGU Mainz) for taking the core pictures of REM 3 and REM 5. Intensive fieldwork conducted by the whole TERRACLIME-Team and associates, namely Aditi Dave (MPI-C, Mainz), Alexandra Nimmrichter (JGU Mainz), Aileen Klinger (JGU Mainz) build the base of this contribution, which we are grateful for.

Appendix A. Supplementary material

Supplementary data to this article can be found online at https://doi.org/10.1016/j.catena.2020.104913.

References

Antoine, P., Coutard, S., Guerin, G., Deschodt, L., Goval, E., Locht, J.-L., Paris, C., 2016. Upper Pleistocene loess-palaeosol records from Northern France in the European context: Environmental background and dating of the Middle Palaeolithic. Quat. Int. 411, 4–24.
Antoine, P., Rousseau, D.-D., Moine, O., Kunesch, S., Hatté, C., Lang, A., Tissoux, H.,

Zöller, L., 2009. Rapid and cyclic aeolian deposition during the Last Glacial in European loess: a high-resolution record from Nussloch, Germany. Quat. Sci. Rev. 28 (25-26), 2955–2973.
Antoine, P., Rousseau, D.-D., Lautridou, J.-P., Hatté, C., 1999. Last interglacial-glacial climatic cycle in loess-palaeosol successions of north-western France. SBOR 28 (4), 551–563.
Antoine, P., Rousseau, D.-D., Zöller, L., Lang, A., Munaut, A.-V., Hatté, C., Fontugne, M., 2001. High-resolution record of the last Interglacial–glacial cycle in the Nussloch loess–palaeosol sequences, Upper Rhine Area, Germany. Quat. Int. 76-77, 211–229.
App, V., Auffermann, B., Hahn, J., Pasda, C., Stephan, E., 1995. Die altsteinzeitliche Fundstelle auf dem Schwalbenberg bei Remagen. Berichte zur Archäologie an Mittelrhein und Mosel 4, 11–136.
Baddouh, M., Meyers, S.R., Carroll, A.R., Beard, B.L., Johnson, C.M., 2016. Lacustrine 87 Sr/ 86 Sr as a tracer to reconstruct Milankovitch forcing of the Eocene hydrologic cycle. Earth Planet. Sci. Lett. 448, 62–68.
Bibus, E., 1980. Zur Relief-. Frankfurter Geowissenschaftliche Arbeiten, Ser. D, Phys. Geogr, Boden- und Sedimententwicklung am unteren Mittelrhein.
Blott, S.J., Croft, D.J., Pye, K., Saye, S.E., Wilson, H.E., 2004. Particle size analysis by laser diffraction. Geol. Soc., London, Special Publications 232 (1), 63–73.
Boenigk, W., Frechen, M., 2006. The Pliocene and Quaternary fluvial archives of the Rhine system. Quat. Sci. Rev. 25 (5-6), 550–574.
Bond, G., Broecker, W., Johnsen, S., McManus, J., Labeyrie, L., Jouzel, J., Bonani, G., 1993. Correlations between climate records from North Atlantic sediments and Greenland ice. Nature 365 (6442), 143–147.
Bosinski, G., 2008. Urgeschichte am Rhein. Kerns.
Buylaert, J.-P., Jain, M., Murray, A.S., Thomsen, K.J., Thiel, C., Sohbati, R., 2012. A robust feldspar luminescence dating method for Middle and Late Pleistocene sediments: Feldspar luminescence dating of Middle and Late Pleistocene sediments. Boreas 41 (3), 435–451.
Cofflet, L., 2005. Paläomagnetische Untersuchungen im Rheinischen Löss.
Cottereau, E., Arnold, M., Moreau, C., Baqué, D., Bavay, D., Caffy, I., Comby, C., Dumoulin, J.-P., Hain, S., Perron, M., Salomon, J., Setti, V., 2007. Artemis, the New 14 C AMS at LMC14 in Saclay, France. Radiocarbon 49 (2), 291–299.
Dansgaard, W., Johnsen, S.J., Clausen, H.B., Dahl-Jensen, D., Gundestrup, N., Hammer, C.U., Oeschger, H., 1984. North Atlantic climatic oscillations revealed by deep Greenland ice cores. Clim. Process. Clim. Sensit. 29, 288–298.
Dansgaard, W., Johnsen, S.J., Clausen, H.B., Dahl-Jensen, D., Gundestrup, N.S., Hammer, C.U., Hvidberg, C.S., Steffensen, J.P., Sveinbjörnsdottir, A.E., Jouzel, J., Bond, G., 1993. Evidence for general instability of past climate from a 250-kyr ice-core record. Nature 364 (6434), 218–220.
Dávila, S.L., Stinnesbeck, S.R., Gonzalez, S., Lindauer, S., Escamilla, J., Stinnesbeck, W., 2019. Guatemala's Late Pleistocene (Rancholabrean) fauna: Revision and interpretation. Quat. Sci. Rev. 219, 277–296.
Duller, G.A.T., 2008. Single-grain optical dating of Quaternary sediments: Why aliquot size matters in luminescence datin. Boreas 37 (4), 589–612. https://doi.org/10.1111/j.1502-3885.2008.00051.x.
Ebisuzaki, W., 1997. A method to estimate the statistical significance of a correlation when the data are serially correlated. J. Clim. https://doi.org/10.1175/1520-0442(1997)010 < 2147:AMTETS > 2.0.CO;2.
Fischer, P., Hambach, U., Klasen, N., Schulte, P., Zeeden, C., Steininger, F., Lehmkuhl, F., Gerlach, R., Radtke, U., 2019. Landscape instability at the end of MIS 3 in western Central Europe: evidence from a multi proxy study on a Loess-Palaeosol-Sequence from the eastern Lower Rhine Embayment, Germany. Quat. Int. 502, 119–136.
Fischer, P., Hilgers, A., Protze, J., Kels, H., Lehmkuhl, F., Gerlach, R., 2012. Formation and geochronology of Last Interglacial to Lower Weichselian loess/palaeosol sequences – case studies from the Lower Rhine Embayment, Germany. E&G Quat. Sci. J. https://doi.org/10.3285/eg.61.1.04.
Fischer, P., Wunderlich, T., Rabbel, W., Vött, A., Willershäuser, T., Baika, K., Rigakou, D., Metallinou, G., 2016. Combined Electrical Resistivity Tomography (ERT), Direct-Push Electrical Conductivity (DP-EC) Logging and Coring - A New Methodological Approach in Geoarchaeological Research: Combining ERT, DP-EC Logs and Coring as New Approach in Geoarchaeology. Archaeol. Prospect. 23 (3), 213–228.
Fitzsimmons, K.E., Marković, S.B., Hambach, U., 2012. Pleistocene environmental dynamics recorded in the loess of the middle and lower Danube basin. Quat. Sci. Rev. 41, 104–118.
Fleitmann, D., Cheng, H., Badertscher, S., Edwards, R.L., Mudelsee, M., Göktürk, O.M., Fankhauser, A., Pickering, R., Raible, C.C., Matter, A., Kramers, J., Tüysüz, O., 2009. Timing and climatic impact of Greenland interstadials recorded in stalagmites from northern Turkey. Geophys. Res. Lett. 36 (19). https://doi.org/10.1029/2009GL040050.
Förster, M.W., Zemlitskaya, A., Otter, L.M., Buhre, S., Sirocko, F., 2020. Late Pleistocene Eifel eruptions: insights from clinopyroxene and glass geochemistry of tephra layers from Eifel Laminated Sediment Archive sediment cores. J. Quaternary Sci. 35 (1-2), 186–198.
Frechen, M., Schirmer, W., 2011. Luminescence Chronology of the Schwalbenberg II Loess in the Middle Rhine Valley. E&G Quat. Sci. J. https://doi.org/10.3285/eg.60.1.05.
Galbraith, R.F., Roberts, R.G., Laslett, G.M., Yoshida, H., Olley, J.M., 1999. Optical dating of single and multiple grains of quartz from Jinmium rock shelter, northern Australia: Part I, experimental design and statistical models. Archaeometry 41, 339–364.
Gocke, M., Hambach, U., Eckmeier, E., Schwark, L., Zöller, L., Fuchs, M., Löscher, M., Wiesenberg, G.L.B., 2014. Introducing an improved multi-proxy approach for paleoenvironmental reconstruction of loess–paleosol archives applied on the Late Pleistocene Nussloch sequence (SW Germany). Palaeogeogr. Palaeoclimatol. Palaeoecol. 410, 300–315.
Grootes, P.M., Stuiver, M., 1997. Oxygen 18/16 variability in Greenland snow and ice with 10 −3 - to 10 5 -year time resolution. J. Geophys. Res. 102 (C12), 26455–26470.
Günther, T., Rücker, C., 2011. Boundless Electrical Resistivity Tomography BERT - the user tutorial. Interface.
Haase, D., Fink, J., Haase, G., Ruske, R., Pécsi, M., Richter, H., Altermann, M., Jäger, K.-D., 2007. Loess in Europe—its spatial distribution based on a European Loess Map, scale 1:2,500,000. Quat. Sci. Rev. 26 (9-10), 1301–1312.
Heinrich, H., 1988. Origin and Consequences of Cyclic Ice Rafting in the Northeast Atlantic Ocean During the Past 130,000 Years. Quat. res. 29 (2), 142–152.
Hemming, S.R., 2004. Heinrich events: Massive late Pleistocene detritus layers of the North Atlantic and their global climate imprint. Rev. Geophys. 42 (1). https://doi.org/10.1029/2003RG000128.
Huntley, D.J., Lamothe, M., 2001. Ubiquity of anomalous fading in K-feldspars and the measurement and correction for it in optical dating. Can. J. Earth Sci. 38 (7), 1093–1106.
JAXA EORC, n.d. ALOS Global Digital Surface Model “ALOS World 3D - 30m” (AW3D30).
Jones, R.M., 2003. Particle size analysis by laser diffraction: ISO 13320, standard operating procedures, and Mie theory. Am. Lab.
Klasen, N., Fischer, P., Lehmkuhl, F., Hilgers, A., 2015. Luminescence dating of loess deposits from the Remagen-Schwalbenberg site, Western Germany. Geochronometria 42. https://doi.org/10.1515/geochr-2015-0008.
Kromer, B., Lindauer, S., Synal, H.-A., Wacker, L., 2013. MAMS – A new AMS facility at the Curt-Engelhorn-Centre for Achaeometry, Mannheim, Germany. Nucl. Instrum. Methods Phys. Res., Sect. B 294, 11–13.
Kukla, G., An, Z., 1989. Loess stratigraphy in Central China. Palaeogeogr. Palaeoclimatol. Palaeoecol. 72, 203–225.
Kukla, G.J., 1977. Pleistocene land—sea correlations I. Europe. Earth Sci. Rev. 13 (4), 307–374.
Lancaster, N., 2020. On the formation of desert loess. Quat. res. 96, 105–122.
Lang, A., Lindauer, S., Kuhn, R., Wagner, G.A., 1996. Procedures of optically and Infrared Stimulated Luminescence Dating of Sediments in Heidelberg. Anc. TL 14, 7–11.
Lehmkuhl, F., Bösken, J., Hošek, J., Sprafke, T., Marković, S.B., Obreht, I., Hambach, U., Sümegi, P., Thiemann, A., Steffens, S., Lindner, H., Veres, D., Zeeden, C., 2018. Loess distribution and related Quaternary sediments in the Carpathian Basin. J. Maps 14 (2), 661–670.
Lehmkuhl, F., Zens, J., Krauß, L., Schulte, P., Kels, H., 2016. Loess-paleosol sequences at the northern European loess belt in Germany: Distribution, geomorphology and stratigraphy. Quat. Sci. Rev. 153, 11–30.
Magyari, E.K., Veres, D., Wennrich, V., Wagner, B., Braun, M., Jakab, G., Karátson, D., Pál, Z., Ferenczy, G.y., St-Onge, G., Rethemeyer, J., Francois, J.-P., von Reumont, F., Schäbitz, F., 2014. Vegetation and environmental responses to climate forcing during the Last Glacial Maximum and deglaciation in the East Carpathians: attenuated response to maximum cooling and increased biomass burning. Quat. Sci. Rev. 106, 278–298.
Marković, S.B., Stevens, T., Kukla, G.J., Hambach, U., Fitzsimmons, K.E., Gibbard, P., Buggle, B., Zech, M., Guo, Z., Hao, Q., Wu, H., O'Hara Dhand, K., Smalley, I.J., Újvári, G., Sümegi, P., Timar-Gabor, A., Veres, D., Sirocko, F., Vasiljević, D.A., Jary, Z., Svensson, A., Jović, V., Lehmkuhl, F., Kovács, J., Svirčev, Z., 2015. Danube loess stratigraphy — Towards a pan-European loess stratigraphic model. Earth Sci. Rev. 148, 228–258.
Marković, S.B., Stevens, T., Mason, J., Vandenberghe, J., Yang, S., Veres, D., Újvári, G., Timar-Gabor, A., Zeeden, C., Guo, Z., Hao, Q., Obreht, I., Hambach, U., Wu, H., Gavrilov, M.B., Rolf, C., Tomić, N., Lehmkuhl, F., 2018. Loess correlations – Between myth and reality. Palaeogeogr. Palaeoclimatol. Palaeoecol. 509, 4–23.
Meyers, S.R., 2014. Astrochron: An R Package for Astrochronology Version 0.8.No Title.
Midwood, A.J., Boutton, T.W., 1998. Soil carbonate decomposition by acid has little effect on δ13C of organic matter. Soil Biol. Biochem. 30 (10-11), 1301–1307.
Moine, O., Antoine, P., Hatté, C., Landais, A., Mathieu, J., Prud’homme, C., Rousseau, D.-D., 2017. The impact of Last Glacial climate variability in west-European loess revealed by radiocarbon dating of fossil earthworm granules. Proc. Natl. Acad. Sci. USA 114 (24), 6209–6214.
Ozer, M., Orhan, M., Isik, N.S., 2010. Effect of Particle Optical Properties on Size Distribution of Soils Obtained by Laser Diffraction. Environ. Eng. Geosci. 16 (2), 163–173.
Pecsi, M., Richter, G., 1995. Loss: Herkunft - Gliederung - Landschaften. Zeitschrift fur Geomorphol, Suppl.
Porter, S.C., Zhisheng, A.n., 1995. Correlation between climate events in the North Atlantic and China during the last glaciation. Nature 375 (6529), 305–308.
Pouclet, A., Juvigné, E., Pirson, S., 2008. The Rocourt Tephra, a widespread 90–74 ka stratigraphic marker in Belgium. Quater. Res. 70 (1), 105–120. https://doi.org/10.1016/j.yqres.2008.03.010.
Preusser, F., Degering, D., Fuchs, M., Hilgers, A., Kadereit, A., Klasen, N., Krbetschek, M., Richter, D., Spencer, J.Q.G., 2008. Luminescence dating: basics, methods and applications. Eiszeitalter Gegenwart / Quat. Sci. J. https://doi.org/10.3285/eg.57.1-2.5.
Profe, J., Zolitschka, B., Schirmer, W., Frechen, M., Ohlendorf, C., 2016. Geochemistry unravels MIS 3/2 paleoenvironmental dynamics at the loess–paleosol sequence Schwalbenberg II, Germany. Palaeogeogr. Palaeoclimatol. Palaeoecol. 459, 537–551.
Prud'homme, C., Lécuyer, C., Antoine, P., Hatté, C., Moine, O., Fourel, F., Amiot, R., Martineau, F., Rousseau, D.-D., 2018. δ 13 C signal of earthworm calcite granules: A new proxy for palaeoprecipitation reconstructions during the Last Glacial in western Europe. Quat. Sci. Rev. 179, 158–166.
Prud'homme, C., Moine, O., Mathieu, J., Saulnier-Copard, S., Antoine, P., 2019. High-resolution quantification of earthworm calcite granules from western European loess sequences reveals stadial-interstadial climatic variability during the Last Glacial. Boreas 48 (1), 257–268.

Rasmussen, S.O., Birks, H.H., Blockley, S.P.E., Brauer, A., Hajdas, I., Hoek, W.Z., Lowe, J.J., Moreno, A., Renssen, H., Roche, D.M., Svensson, A.M., Valdes, P., Walker, M.J.C., 2014. Dating, synthesis, and interpretation of palaeoclimatic records of the Last Glacial cycle and model-data integration: advances by the INTIMATE (INTegration of Ice-core, MArine and TErrestrial records) COST Action ES0907. Quat. Sci. Rev. 106, 1–13.

Reimer, P.J., Bard, E., Bayliss, A., Beck, J.W., Blackwell, P.G., Ramsey, C.B., Buck, C.E., Cheng, H., Edwards, R.L., Friedrich, M., Grootes, P.M., Guilderson, T.P., Haflidason, H., Hajdas, I., Hatté, C., Heaton, T.J., Hoffmann, D.L., Hogg, A.G., Hughen, K.A., Kaiser, K.F., Kromer, B., Manning, S.W., Niu, M.u., Reimer, R.W., Richards, D.A., Scott, E.M., Southon, J.R., Staff, R.A., Turney, C.S.M., van der Plicht, J., 2013. IntCal13 and Marine13 Radiocarbon Age Calibration Curves 0–50,000 Years cal BP. Radiocarbon 55 (4), 1869–1887.

Reimer, P.J., Brown, T.A., Reimer, R.W., 2004. Discussion: Reporting and calibration of post-bomb 14C data. Radiocarbon. https://doi.org/10.1017/S0033822200033154.

Rousseau, D.-D., Derbyshire, E., Antoine, P., Hatté, C., 2018. In: Reference Module in Earth Systems and Environmental Sciences. Elsevier. https://doi.org/10.1016/B978-0-12-409548-9.11136-4.

Rousseau, D.D., Svensson, A., Bigler, M., Sima, A., Steffensen, J.P., Boers, N., Peder Steffensen, J., Boers, N., 2017a. Eurasian contribution to the last glacial dust cycle: how are loess sequences built? Clim. Past Discuss. https://doi.org/10.5194/cp-2017-67.

Rousseau, D.D., Boers, N., Sima, A., Svensson, A., Bigler, M., Lagroix, F., Taylor, S., Antoine, P., 2017b. (MIS3 & 2) millennial oscillations in Greenland dust and Eurasian aeolian records – A paleosol perspective. Quat. Sci. Rev. https://doi.org/10.1016/j.quascirev.2017.05.020.

Rousseau, D.-D., Chauvel, C., Sima, A., Hatté, C., Lagroix, F., Antoine, P., Balkanski, Y., Fuchs, M., Mellett, C., Kageyama, M., Ramstein, G., Lang, A., 2014. European glacial dust deposits: Geochemical constraints on atmospheric dust cycle modeling: European Glacial Dust Deposits. Geophys. Res. Lett. 41 (21), 7666–7674.

Rousseau, D.-D., Sima, A., Antoine, P., Hatté, C., Lang, A., Zöller, L., 2007. Link between European and North Atlantic abrupt climate changes over the last glaciation. Geophys. Res. Lett. 34 (22). https://doi.org/10.1029/2007GL031716.

Sakai, K., Peltier, W.R., 1999. A dynamical systems model of the Dansgaard-Oeschger oscillation and the origin of the bond cycle. J. Clim. https://doi.org/10.1175/1520-0442(1999)012 < 2238:adsmot > 2.0.co;2.

Schaetzl, R.J., Bettis III, E.A., Crouvi, O., Fitzsimmons, K.E., Grimley, D.A., Hambach, U., Lehmkuhl, F., Marković, S.B., Mason, J.A., Owczarek, P., Roberts, H.M., Rousseau, D.-D., Stevens, T., Vandenberghe, J., Zárate, M., Veres, D., Yang, S., Zech, M., Conroy, J.L., Dave, A.K., Faust, D., Hao, Q., Obreht, I., Prud'homme, C., Smalley, I., Tripaldi, A., Zeeden, C., Zech, R., 2018. Approaches and challenges to the study of loess—Introduction to the LoessFest Special Issue. Quat. res. 89 (3), 563–618.

Schiermeyer, J., 2000. Würmzeitliche Lößmollusken aus der Eifel.

Schirmer, W., 2000. Eine Klimakurve des Oberpleistozäns aus dem rheinischen Löss. Eiszeitalter und Gegenwart.

Schirmer, W., 2016. Late Pleistocene loess of the Lower Rhine. Quat. Int. 411, 44–61.

Schirmer, W., 2012. Rhine loess at Schwalbenberg II – MIS 4 and 3. E&G Quat. Sci. J. https://doi.org/10.3285/eg.61.1.03.

Schirmer, W., 1991. Würmzeitliche Böden am Mittelrhein. 10. Tagung des AK Paläoböden der DBG, Program. und Exkursionsführer 70–83.

Schirmer, W., Ikinger, A., Nehring, F., 2012. Die terrestrischen Böden im Profil Schwalbenberg/Mittelrhein. Mainzer Geowissenschaftliche Mitteilungen.

Schlummer, M., Hoffmann, T., Dikau, R., Eickmeier, M., Fischer, P., Gerlach, R., Holzkämper, J., Kalis, A.J., Kretschmer, I., Lauer, F., Maier, A., Meesenburg, J., Meurers-Balke, J., Münch, U., Pätzold, S., Steininger, F., Stobbe, A., Zimmermann, A., 2014. From point to area: Upscaling approaches for Late Quaternary archaeological and environmental data. Earth Sci. Rev. 131, 22–48.

Schulte, P., Lehmkuhl, F., Steininger, F., Loibl, D., Lockot, G., Protze, J., Fischer, P., Stauch, G., 2016. Influence of HCl pretreatment and organo-mineral complexes on laser diffraction measurement of loess–paleosol-sequences. CATENA 137, 392–405.

Shackleton, N.J., 1987. Oxygen isotopes, ice volume and sea level. Quat. Sci. Rev. 6 (3-4), 183–190.

Sirocko, F., 2016. The ELSA - Stacks (Eifel-Laminated-Sediment-Archive): An introduction. Global Planet. Change 142, 96–99.

Sirocko, F., Knapp, H., Dreher, F., Förster, M.W., Albert, J., Brunck, H., Veres, D., Dietrich, S., Zech, M., Hambach, U., Röhner, M., Rudert, S., Schwibus, K., Adams, C., Sigl, P., 2016. The ELSA-Vegetation-Stack: Reconstruction of Landscape Evolution Zones (LEZ) from laminated Eifel maar sediments of the last 60,000 years. Glob. Planet. Change 142, 108–135. https://doi.org/10.1016/J.GLOPLACHA.2016.03.005.

Smalley, I.J., Kumar, R., O'Hara Dhand, K., Jefferson, I.F., Evans, R.D., 2005. The formation of silt material for terrestrial sediments: Particularly loess and dust. Sed. Geol. 179 (3-4), 321–328.

Sprafke, T., Fitzsimmons, K.E., Grützner, C., Elliot, A., Marquer, L., Nigmatova, S., 2018. Reevaluation of Late Pleistocene loess profiles at Remizovka (Kazakhstan) indicates the significance of topography in evaluating terrestrial paleoclimate records. Quat. res. 89 (3), 674–690.

Sprafke, T., Obreht, I., 2016. Loess: Rock, sediment or soil – What is missing for its definition? Quat. Int. 399, 198–207.

Street, M., Baales, M., Cziesla, E., Hartz, S., Heinen, M., Jöris, O., Koch, I., Pasda, C., Terberger, T., Vollbrecht, J., 2001. Final paleolithic and mesolithic research in reunified Germany. J. World Prehistory. https://doi.org/10.1023/A:1014332527763.

Stuiver, M., Polach, H.A., 1977. Discussion Reporting of 14 C Data. Radiocarbon 19 (3), 355–363.

Thiel, C., Buylaert, J.-P., Murray, A., Terhorst, B., Hofer, I., Tsukamoto, S., Frechen, M., 2011. Luminescence dating of the Stratzing loess profile (Austria) – Testing the potential of an elevated temperature post-IR IRSL protocol. Quat. Int. 234 (1-2), 23–31.

Veres, D., Lallier-Vergès, E., Wohlfarth, B., Lacourse, T., Kéravis, D., Björck, S., Preusser, F., Andrieu-Ponel, V., Ampel, L., 2009. Climate-driven changes in lake conditions during late MIS 3 and MIS 2: A high-resolution geochemical record from Les Echets, France. Boreas. https://doi.org/10.1111/j.1502-3885.2008.00066.x.

Vinnepand, M., Fischer, P., Fitzsimmons, K., Thornton, B., Fiedler, S., Vött, A., 2020. Combining Inorganic and Organic Carbon Stable Isotope Signatures in the Schwalbenberg Loess-Palaeosol-Sequence Near Remagen (Middle Rhine Valley, Germany). Front. Earth Sci. 8. https://doi.org/10.3389/feart.2020.00276.

Wacker, L., Fülöp, R.-H., Hajdas, I., Molnár, M., Rethemeyer, J., 2013. A novel approach to process carbonate samples for radiocarbon measurements with helium carrier gas. Nucl. Instrum. Methods Phys. Res., Sect. B 294, 214–217.

Wang, Y.J., Cheng, H., Edwards, R.L., An, Z.S., Wu, J.Y., Shen, C.C., Dorale, J.A., 2001. A high-resolution absolute-dated late pleistocene monsoon record from Hulu Cave, China. Science 80-. https://doi.org/10.1126/science.1064618.

Weninger, B., Jöris, O., 2008. A 14C age calibration curve for the last 60 ka: the Greenland-Hulu U/Th timescale and its impact on understanding the Middle to Upper Paleolithic transition in Western Eurasia. J. Hum. Evol. 55 (5), 772–781.

Wolff, E.W., Chappellaz, J., Blunier, T., Rasmussen, S.O., Svensson, A., 2010. Millennial-scale variability during the last glacial: The ice core record. Quat. Sci. Rev. 29 (21-22), 2828–2838.

Wunderlich, T., Fischer, P., Wilken, D., Hadler, H., Erkul, E., Mecking, R., Günther, T., Heinzelmann, M., Vött, A., Rabbel, W., 2018. Constraining electric resistivity tomography by direct push electric conductivity logs and vibracores: An exemplary study of the Fiume Morto silted riverbed (Ostia Antica, western Italy). Geophysics 83 (3), B87–B103.

Zazzo, A., Saliège, J.-F., 2011. Radiocarbon dating of biological apatites: A review. Palaeogeogr. Palaeoclimatol. Palaeoecol. 310 (1-2), 52–61.

Zens, J., Schulte, P., Klasen, N., Krauß, L., Pirson, S., Burow, C., Brill, D., Eckmeier, E., Kels, H., Zeeden, C., Spagna, P., Lehmkuhl, F., 2018. OSL chronologies of paleoenvironmental dynamics recorded by loess-paleosol sequences from Europe: Case studies from the Rhine-Meuse area and the Neckar Basin. Palaeogeogr. Palaeoclimatol. Palaeoecol. 509, 105–125.

Zens, J., Zeeden, C., Römer, W., Fuchs, M., Klasen, N., Lehmkuhl, F., 2017. The Eltville Tephra (Western Europe) age revised: Integrating stratigraphic and dating information from different Last Glacial loess localities. Palaeogeogr. Palaeoclimatol. Palaeoecol. 466, 240–251.

Zöller, L., Conard, N.J., Hahn, J., 1991. Thermoluminescence dating of middle palaeolithic open air sites in the Middle Rhine Valley/Germany. Naturwissenschaften 78 (9), 408–410.

Zöller, L., Semmel, A., 2001. 175 years of loess research in Germany—long records and "unconformities". Earth Sci. Rev. 54 (1-3), 19–28.